Neurosci. Bull. December, 2023, 39(12):1789–1806
https://doi.org/10.1007/s12264-023-01075-0

www.neurosci.cn
www.springer.com/12264

ORIGINAL ARTICLE

Peripheral BDNF Regulates Somatosensory–Sympathetic Coupling in Brachial Plexus Avulsion-Induced Neuropathic Pain

Hang Xian[1] · Huan Guo[2,4] · Yuan-Ying Liu[3,4] · Jian-Lei Zhang[1] · Wen-Chao Hu[4,5] · Ming-Jun Yu[6] · Rui Zhao[1] · Rou-Gang Xie[4] · Hang Zhang[1] · Rui Cong[1]

Received: 13 November 2022 / Accepted: 19 March 2023 / Published online: 19 June 2023

Abstract Brachial plexus avulsion (BPA) is a combined injury involving the central and peripheral nervous systems. Patients with BPA often experience severe neuropathic pain (NP) in the affected limb. NP is insensitive to the existing treatments, which makes it a challenge to researchers and clinicians. Accumulated evidence shows that a BPA-induced pain state is often accompanied by sympathetic nervous dysfunction, which suggests that the excitation state of the sympathetic nervous system is correlated with the existence of NP. However, the mechanism of how somatosensory neural crosstalk with the sympathetic nerve at the peripheral level remains unclear. In this study, through using a novel BPA C7 root avulsion mouse model, we found that the expression of BDNF and its receptor TrκB in the DRGs of the BPA mice increased, and the markers of sympathetic nervous system activity including α1 and α2 adrenergic receptors (α1-AR and α2-AR) also increased after BPA. The phenomenon of superexcitation of the sympathetic nervous system, including hypothermia and edema of the affected extremity, was also observed in BPA mice by using CatWalk gait analysis, an infrared thermometer, and an edema evaluation. Genetic knockdown of BDNF in DRGs not only reversed the mechanical allodynia but also alleviated the hypothermia and edema of the affected extremity in BPA mice. Further, intraperitoneal injection of adrenergic receptor inhibitors decreased neuronal excitability in patch clamp recording and reversed the mechanical allodynia of BPA mice. In another branch experiment, we also found the elevated expression of BDNF, TrκB, TH, α1-AR, and α2-AR in DRG tissues from BPA patients compared with normal human DRGs through western blot and immunohistochemistry. Our results revealed that peripheral BDNF is a key molecule in the regulation of somatosensory-sympathetic coupling in BPA-induced NP. This study also opens a novel analgesic target (BDNF) in the treatment of this pain with fewer complications, which has great potential for clinical transformation.

Hang Xian, Huan Guo and Yuan-Ying Liu have contributed equally to this work.

Supplementary Information The online version contains supplementary material available at https://doi.org/10.1007/s12264-023-01075-0.

✉ Rou-Gang Xie
rgxie@fmmu.edu.cn

✉ Hang Zhang
zhanghang1983@163.com

✉ Rui Cong
congrui@fmmu.edu.cn

[1] Department of Orthopedics, Xijing Hospital, The Air Force Medical University, Xi'an 710032, China

[2] Pain and Related Diseases Research Laboratory, Medical College of Shantou University, Shantou 515041, China

[3] School of Life Science and Research Center for Resource Peptide Drugs, Shaanxi Engineering and Technological Research Center for Conversation and Utilization of Regional Biological Resources, Yanan University, Yanan 716000, China

[4] Department of Neurobiology, School of Basic Medicine, The Air Force Medical University, Xi'an 710032, China

[5] The Sixth Regiment, School of Basic Medicine, The Air Force Medical University, Xi'an 710032, China

[6] The Tenth Squadron of the Third Regiment, School of Basic Medicine, The Air Force Medical University, Xi'an 710032, China

Keywords Brachial plexus avulsion · Neuropathic pain · Sympathetic nervous system · Brain-derived neurotrophic factor · Peripheral sensitization · Mechanical allodynia

Introduction

Brachial plexus avulsion (BPA) is the most devastating injury of the upper extremity, which results from single or multiple nerve roots avulsed from the spinal cord of the brachial plexus due to severe separation injury of the head, neck, shoulder, and upper extremity [1]. It is a combined injury involving the central and peripheral nervous systems. One major consequence of BPA is neuropathic pain (NP), which affects up to 90% of BPA patients according to epidemiological data [2]. BPA-induced NP is often characterized by spontaneous pain, allodynia, and/or hyperalgesia during the course of the disease [3, 4]. The gradual chronic transformation of the pain and the lack of effective treatment methods make it a thorny issue for researchers and clinicians. Therefore, understanding and unveiling the mechanism of BPA-induced NP is a prerequisite for developing a treatment strategy.

As pain sensitization plays a crucial role in the initiation and maintenance of NP, peripheral sensitization is considered to be the priming factor during pain development [5–7]. An increasing number of studies have shown that primary sensory neurons in the dorsal root ganglion (DRG) participate in the occurrence and maintenance of neuropathic pain, and targeting DRG neurons at the peripheral level can achieve pain relief [8–11]. The sympathetic nervous system (SNS) is a part of the autonomic nervous system, and activation of the SNS has wide effects including the cardiac, pulmonary, urinary, and digestive systems, as well as perspiration [12]. Recently, accumulating preclinical and clinical evidence has shown crosstalk between the somatosensory nervous system and the SNS under pathological situations, and pain conditions can be exacerbated by SNS activity at the peripheral level [13–15]. The reported anatomical basis of this somatosensory-sympathetic coupling is sympathetic fibers sprouting into the DRG and forming a basket structure around neurons. This abnormal innervation could enhance the activity of nociceptors through direct norepinephrine (NE) release from sympathetic nerves and increase the expression of α-adrenergic receptors (α-ARs) in the DRG [16–18]. In the clinic, BPA patients often experience persistent pain combined with hypothermia, edema, and abnormal sweating of the affected extremity, which strongly suggests that the SNS takes part in the BPA-induced NP condition. However, the mechanism underlying this pathological process is still unknown.

Neurotrophins, including nerve growth factor (NGF), brain-derived neurotrophic factor (BDNF), and glial-derived neurotrophic factor (GDNF), have been demonstrated to be involved in the regulation of NP after a variety of different types of nerve injury [19, 20]. NGF has been shown to regulate the structural and functional remodeling of sympathetic nerve fibers after NP, and it can mediate the increased expression of BDNF in the DRG under inflammation-induced pain [20]. As for BPA injury, the avulsed roots have lost contact with the spinal cord, and how the DRGs take part in NP development and their role in peripheral sensitization is still unclear. In this study, we used a well-designed BPA mouse model of NP, focusing on peripheral BDNF, to explore its function in the regulation of somatosensory-sympathetic coupling under BPA-induced NP conditions and further investigate the underlying mechanisms in both mouse and human DRGs.

Materials and Methods

Animals

Adult female C57BL/6 mice (20−30 g) were housed in a temperature-controlled environment with a standard 12/12-h dark/light cycle and were allowed free access to food and water throughout the experimental protocol. All the animal procedures were approved by the Animal Care Committee of the Air Force Medical University.

BPA Modeling Procedures

C57BL/6 mice were anesthetized by intraperitoneal (i.p.) injection of 1% pentobarbital sodium. A horizontal incision below the left clavicle that runs from the sternum to the axillary region was selected. After the separation of the pectoralis major muscle, deep dissection was performed to expose the brachial plexus in the anterior border space of the pectoralis minor muscle. The middle trunk (C7 root) of the brachial plexus was carefully dissected. A soft silk thread was used to hook the C7 nerve root and the thread was pulled with constant traction toward the distal limb to mimic the mechanism of root avulsion injury. Then, the C7 nerve root where the DRG body could be seen was avulsed (Fig. 1A). In the sham group, the brachial plexus was only exposed and dissected without any further lesions to the nerves. Tissue layers and skin were finally sutured with 4–0 silk.

Behavioral Analysis and Evaluation of Sympathetic Nerve Function

Before testing, mice were allowed to acclimatize to the behavioral tests room for at least 3 days, and all mice were

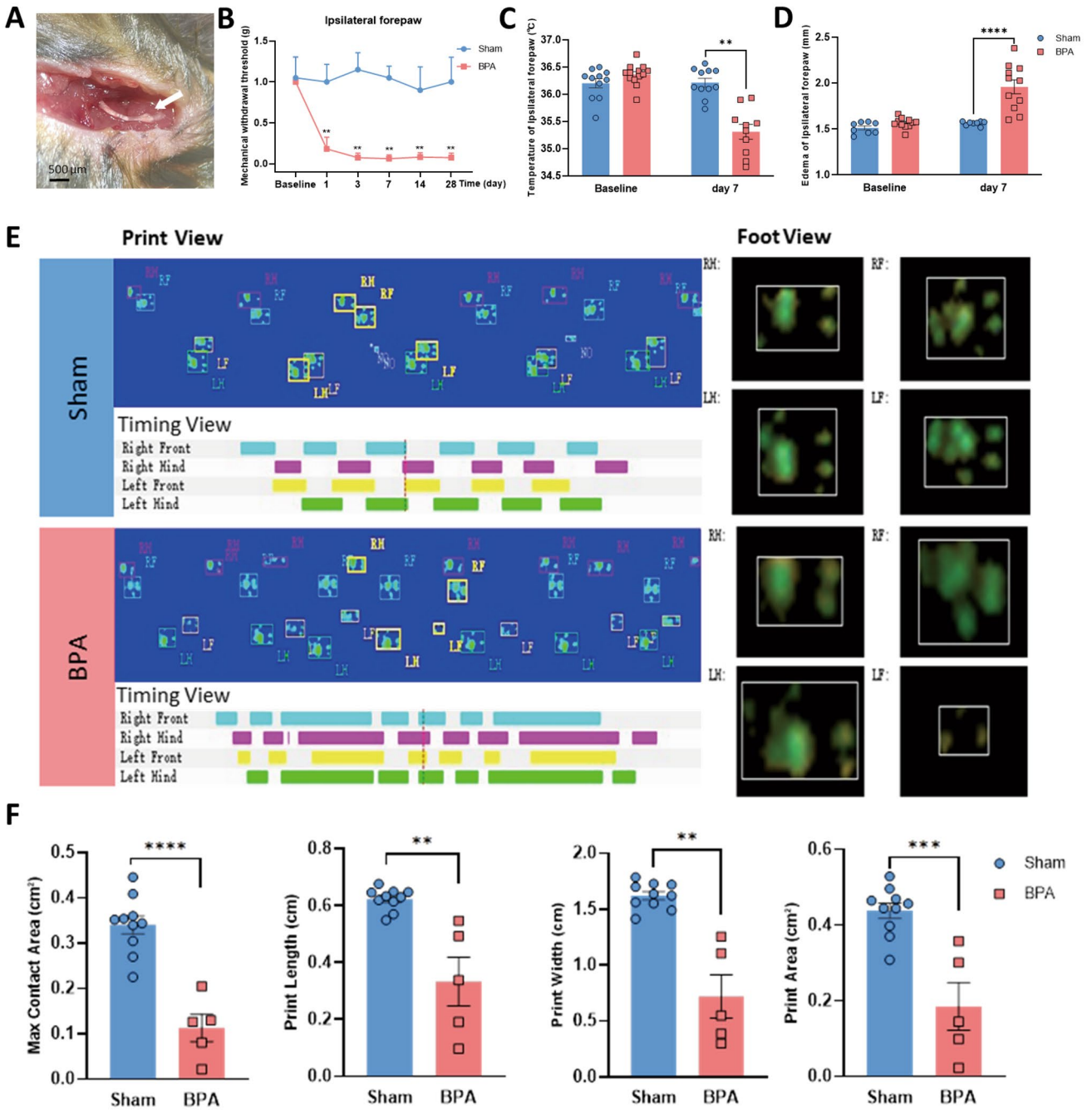

Fig. 1 BPA-induced mechanical allodynia in mice is accompanied by symptoms of sympathetic nerve hyperexcitation. **A** Appearance of the avulsed C7 nerve root with the DRG soma (white arrow). **B** Mechanical allodynia of the ipsilateral forepaw of BPA mice shows a decreased threshold on days 1, 3, 7, 14, and 28 after BPA, $n = 8$. **C** Temperature of the ipsilateral forepaw shows a decrease on day 7 after BPA. **D** Edema occurs on day 7 after BPA. **E** Representative images of CatWalk gait including print view, timing view, and foot view of sham and BPA models. **F** BPA induces a significant decrease in the max contact area, print length, print width, and print area, due to pain and edema of the ipsilateral forepaw. Data are presented as the mean ± SEM. $^{**}P < 0.01$, $^{***}P < 0.001$, $^{****}P < 0.0001$, *vs.* Sham. RF, right forepaw; RH, right hind paw; LF, left forepaw; LH, left hind paw.

randomly allocated to the experimental groups. Mice were accommodated in individual test compartments for at least 1 h before testing and all the behavioral tests were completed by the same experimenter in a blinded manner.

Mechanical Allodynia

Mechanical allodynia (mechanical withdrawal threshold testing) was tested by using a series of von Frey filaments

ranging from 0.008 g to 2.0 g (0.008 g, 0.02 g, 0.04 g, 0.07 g, 0.16 g, 0.4 g, 0.6 g, 1.0 g, 1.4 g, and 2.0 g) on an elevated mesh-bottomed platform (Danamic Globe, USA). Starting with 0.008 g, von Frey filaments were applied to stimulate the plantar surface of the left forepaw. Positive responses to the stimulation included rapid flicking and/or biting, licking, and shaking of the paw while excluding walking movements. Each filament was applied 10 times, and the positive paw response frequency was recorded. The force of a particular filament required to elicit a 50% frequency of paw withdrawal was expressed as the mechanical threshold.

CatWalk Gait Analysis

Mice were trained on an enclosed glass platform at least 3 times each day before gait analysis began. Gait analysis has proven to be a reliable method for measuring pain-related behaviors [21–23]. The mouse was placed on the open end of the glass plate and walked across the whole glass floor voluntarily, and a high-speed camera under the platform captured the image of each footprint and transmitted the recorded data to gait analysis software (CatWalk XT, version 10.6; Noldus, Netherlands). Parameters including max contact area (cm^2, as the maximum print area during paw contact with the glass plate), print length (cm, as the horizontal length of the whole paw print), print width (cm, as the vertical width of the whole paw print), print area (cm^2, the surface area of the whole print), stand (s, the duration in seconds of the paw touching the plate), max contact mean intensity (the mean intensity of the max paw contact), body speed (cm/s), and run average speed (cm/s) were finally analyzed to evaluate the degree of pain and edema of the affected paw (left forepaw).

Forepaw Temperature Evaluation

Temperature measurements of each mouse's left forepaw were taken at various time points after BPA or sham operation. The procedure was applied to the ventral surface of the paw using a digital contactless infrared thermometer in a constant temperature room. The temperature of each paw was measured 3 times and the mean temperature was recorded and analyzed.

Forepaw Edema Evaluation

Edema of the mouse's left forepaw was measured by using a digital Vernier caliper at various time points after BPA or sham operation as previously reported [24]. The thickness of the forepaw was measured. Mice were carefully handled, and the caliper was placed in contact with forepaw skin without pressure. The edema of each paw was measured 3 times and the mean thickness was recorded and analyzed.

Western Blot Analysis

Seven days after the sham and BPA operations, DRG tissues were dissected from the sham group (containing left C6–C8 DRGs) and the BPA group (containing left C6 and C8 DRGs and avulsed C7 roots) and lysed in RIPA lysis buffer (50 mmol/L Tris-HCl, pH 7.4, 150 mmol/L NaCl, 5 mmol/L EDTA, 1% Triton X-100, 0.5% sodium deoxycholate, 0.1% SDS) with protease inhibitors on ice. Protein concentration was measured by BCA Protein Assay Kit (Thermo Scientific, USA) and mixed with 5× loading buffer (CWBIO, China), then heated at 98°C for 10 min. Protein samples were loaded and resolved by SDS-PAGE. Primary antibodies including rabbit anti-BDNF (1:1000, SAB, USA), goat anti-TrκB (1:800, R&D systems, USA), rabbit anti-TH (1:800, CST, USA), rabbit anti-α1-AR (1:1000, Thermo Scientific, USA), rabbit anti-α2-AR (1:1000, Thermo Scientific, USA), rabbit anti-β-actin (1:2000, Proteintech, USA) and rabbit anti-GAPDH (1:2000, Proteintech, USA) were incubated at 4°C overnight. After immunoblotting with the corresponding secondary antibodies at room temperature for 2 h, proteins were visualized using an enhanced chemiluminescence detection method. The captured images were quantified using ImageJ software (V1.6, USA). Specific bands for each protein were normalized to their respective β-actin or GAPDH.

Immunofluorescence Labeling and Cell Counting

Mice were anesthetized by intraperitoneal (i.p.) injection of 1% pentobarbital sodium and transcardially perfused with saline (20 mL) followed by 4% paraformaldehyde (PFA, 20 mL) at day 7 after the sham and BPA operations. As for western blotting above, the left cervical DRGs of each group were removed and post-fixed overnight in 4% PFA and then immersed in 30% sucrose at 4°C until they sank to the bottom of the container. In brief, serial sections were cut at 12 μm on a cryostat and immunostained with primary antibodies including goat anti-BDNF (1:400, Everest Biotech, UK), goat anti-TrκB (1:800, R&D systems, USA), rabbit anti-TH (1:200, CST, USA), rabbit anti-α1-AR (1:400, Thermo Scientific, USA), rabbit anti-α2-AR (1:400, Thermo Scientific, USA), mouse anti-CGRP (1:1000, Abcam, UK), and isolectin B4 (IB4, 1:300, Vector, USA) at 4°C overnight. Secondary antibodies, including Alexa Fluor 594 (donkey anti-goat IgG, 1:1000, Abcam, UK), Alexa Fluor 488 (goat anti-rabbit IgG, 1:1000, Abcam, UK), and Streptavidin Alexa Fluor 647 (1:1000, Solarbio, China), were incubated at room temperature for 4 h. The nuclei were stained by DAPI (1:2000). All images were captured under an Olympus

confocal microscope (Olympus FV3000, Japan). Captured images at a 20× magnification under this confocal microscope were processed using ImageJ, and cell counts were made manually in at least 8 sections from 3 to 5 animals and 4 sections from humans. All counts were conducted blinded to the experimental group.

Injection of rAAV Carrying shRNA into DRGs and Medication Delivery

Mice were anesthetized by i.p. injection of 1% pentobarbital sodium and placed on a standard brain stereoscopic locator (RWD, China). Left C6–C8 DRGs were exposed through a longitudinal incision made on the back of the neck. The epineurium over the DRG was dissected and a microsyringe with a glass pipette was inserted into the ganglion to a depth of 100 μm−150 μm from the surface of the ganglion. 700 nL of virus solution was injected at 70 nL/min using a microprocessor-controlled minipump into the C6, C7, and C8 DRGs. The pipette was removed from the ganglion after a further delay of 10 min. The paravertebral muscles and skin layer were carefully sutured and mice were allowed to recover on a 37°C warming blanket. Mice were allowed to recover for 3 weeks before behavioral analysis and DRG patch-clamp recording (Figs. 4A, 5A). rAAV (synthesized by BrainVTA, Wuhan, China) carried BDNF knockdown shRNA (rAAV2/8-U6-shRNA (BDNF)-CMV-EGFP-SV40 pA) and control rAAV (rAAV2/8-U6-shRNA(scramble)-CMV-EGFP-SV40 pA) were used in the study protocol. The BDNF high-affinity tropomyosin-related kinase B receptor (TrκB) antagonist ANA-12 (MCE, China) and the α-AR antagonist phentolamine (MCE, China) were injected i.p. into mice at 0.5 mg/kg and 1 mg/kg respectively, and the same dose of the vehicle was used in the control group. These antagonists were first administered 7 days after BPA, and then once a day for 5 consecutive days. Then the behavioral analysis was conducted (Figs. 6A, 7A).

DRG Patch-clamp Recording

Mice were anesthetized and whole DRGs were removed from the sham group (containing the left C6–C8 DRGs) and the BPA group (containing the left C6 and C8 DRGs, similar in the rAAV injection groups). The epineurium over the DRG was dissected under microscopy and then incubated in trypsin solution for 15 min at 37°C. The prepared DRG tissue was incubated in the incubation solution (in mmol/L: NaCl, 95; KCl, 1.8; KH_2PO_4, 1.2; $CaCl_2$, 0.5; $MgSO_4$, 7; $NaHCO_3$, 26; glucose, 15; pH 7.4) at room temperature until use. The incubation solution was saturated with 95% O_2 and 5% CO_2 at 26°C for at least 1 h−3 h before the experiment. DRG tissue was then transferred into a recording chamber and superfused with an oxygenated recording solution at 2 mL/min at room temperature. The recording solution was identical to the incubation solution except for (in mmol/L): NaCl 127, $CaCl_2$ 2.4, $MgSO_4$ 1.3, and glucose 0. Standard whole-cell patch clamp recordings were made with glass pipettes having a resistance of 3 MΩ−5 MΩ. The composition of the pipette internal solution was (in mmol/L): KCl 18; K-Glu 120; $CaCl_2$ 1; $MgCl_2$ 2; EGTA 1.1; HEPES 10; Mg-ATP 5; pH 7.4. DRG neurons were visualized with a 40× water-immersion objective using a microscope (BX51WI; Olympus, Tokyo, Japan) equipped with infrared differential interference contrast optics. Whole-cell current and voltage recordings were acquired with a HEKA EPC-10 USB amplifier (HEKA Elektronik, Germany) and PatchMaster software. Signals were low-pass filtered at 5 kHz, sampled at 10 kHz, and analyzed offline. Cells with a clear outline and no membranous tissue coverage were selected as target cells for recording under a high-magnification microscope (Leica, Germany). Neurons carrying green fluorescence in the rAAV groups were selected as target cells for recording. After entering a stable patch-clamp recording mode, the following parameters of the neurons were recorded: resting membrane potential (RMP), membrane resistance (Rm), membrane capacitance (Cm), and access resistance (Ra). Specific parameters were selected to evaluate the cell excitability (Clampfit 10.7, USA) and statistical analysis was applied. The TrκB antagonist ANA-12 and the α-AR antagonist phentolamine were used at the concentration of 10 μmol and 100 μmol in the recording protocol to test their effect on the excitability of the targeted neurons.

Human DRG Tissues

Human DRG tissues were harvested from BPA patients who were admitted to our hospital. The inclusion criteria included adult patients who suffered from chronic pain for >3 months after BPA. Neuropathic pain was suffered by most BPA patients, especially those with root avulsion. A series of reconstruction surgical procedures are needed to treat BPA, including partial resection of the avulsed nerve roots (including the DRG cell bodies) and then nerve anastomosis for the recovery of function of the affected limb. The intraoperative resected avulsed nerve roots (including DRG cell bodies) of the brachial plexus were collected and further biochemical tests (western blot analysis and immunofluorescence labeling, similar to above) were conducted. Normal human DRG tissues were donated by the tissue bank of the Orthopedics Department. The study was approved by the Ethics Committee of Xijing Hospital, the Air Force Medical University. Patients involved in this study signed informed consent forms, and all specimens

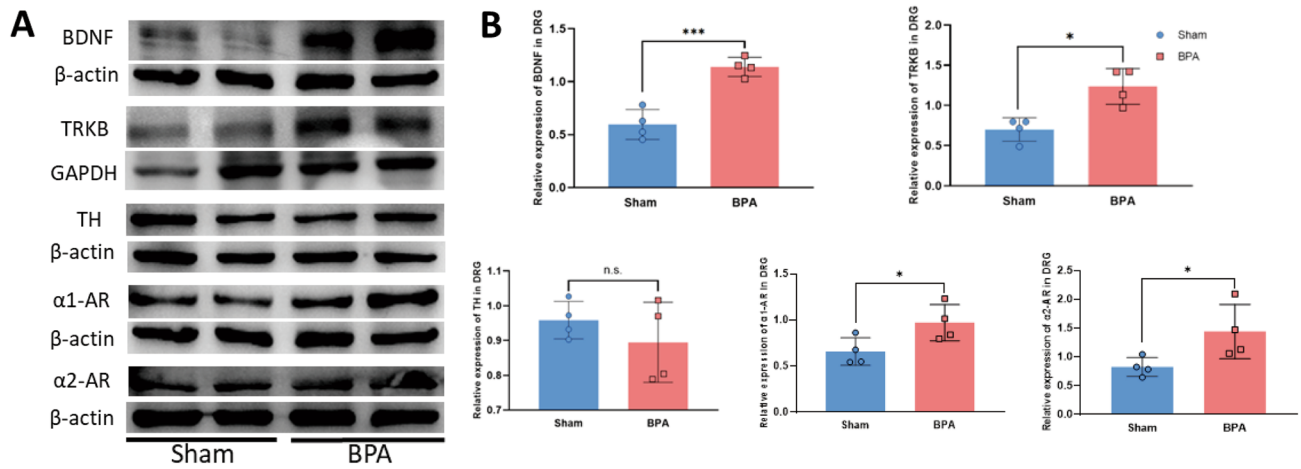

Fig. 2 BPA-induced molecular changes include increased expression of NP markers (BDNF and TrκB) and SNS activity markers (TH, α1-AR, and α2-AR) in the ipsilateral DRGs of mice. **A** Typical examples of western blots showing BDNF, TrκB, TH, α1-ARs, and α2-ARs in the DRG tissue of the sham and BPA mice. **B** BPA increases the expression of BDNF, TrκB, α1-ARs, and α2-ARs in the DRG of mice but not that of TH. Data are normalized to the housekeeping protein β-actin or GAPDH. Data are presented as the mean ± SEM. $*P < 0.05$, $**P < 0.01$, $***P < 0.001$, *vs.* Sham. n.s.: no significant difference.

were handled in an anonymized way according to ethical and legal standards.

Data Analysis and Statistics

All statistical analyses were performed in GraphPad Prism 8.0 and SPSS 21.0 software. Data are presented as the mean ± SEM. Data that met Tukey's and Bonferroni's tests were analyzed using the two-tailed, unpaired, or paired *t*-test, one-way ANOVA, or repeated-measures ANOVA followed by Tukey's multiple-comparison test. Unless otherwise specified, the *P* values shown in figures and text are derived from the analysis of variance. $P < 0.05$ was considered a significant difference.

Results

BPA-Induced Mechanical Allodynia of the Affected Forepaw and Hyper-Excitation of the Sympathetic Nerve

Following left C7 root avulsion of the brachial plexus, the mice showed persistent mechanical allodynia of the affected forepaw and ipsilateral hind paw that started from day 1 and lasted until day 28 after BPA (Figs. 1B, S1B). The pain state was directly assessed in the affected forepaw in this novel model compared with other reported BPA models [2, 25]. This long-lasting pain behavior also met the requirements of the following experiments. As hypothermia and edema are common symptoms of sympathetic nerve hyperexcitability, we analyzed gait, temperature, and edema to assess sympathetic nerve activity. The results showed the temperature of the affected forepaw decreased on day 7 after BPA and the edema occurred at the same time, which was significantly different from the sham group (Figs. 1C, D and S1A). The gait analysis showed the max contact area, print length, print width, and print area decreased during the same time interval after BPA and was significantly different from the sham group (Fig. 1E, F). We consider the decrease of the above indices of gait analysis to be the combined results of pain and edema and are an indirect but reliable index of edema. Meanwhile, the parameters stand, max contact mean intensity, body speed, and run average speed did not significantly differ from the sham group (Fig. S1C). The above results indicated that the SNS activity was activated following the onset of NP after BPA. Unchanged body speed and run average speed also indicated that single root avulsion of C7 did not affect the motor function of the BPA mice, and the assessment of pain state through direct stimulation of the affected forepaw was a reliable way to evaluate the degree of pain.

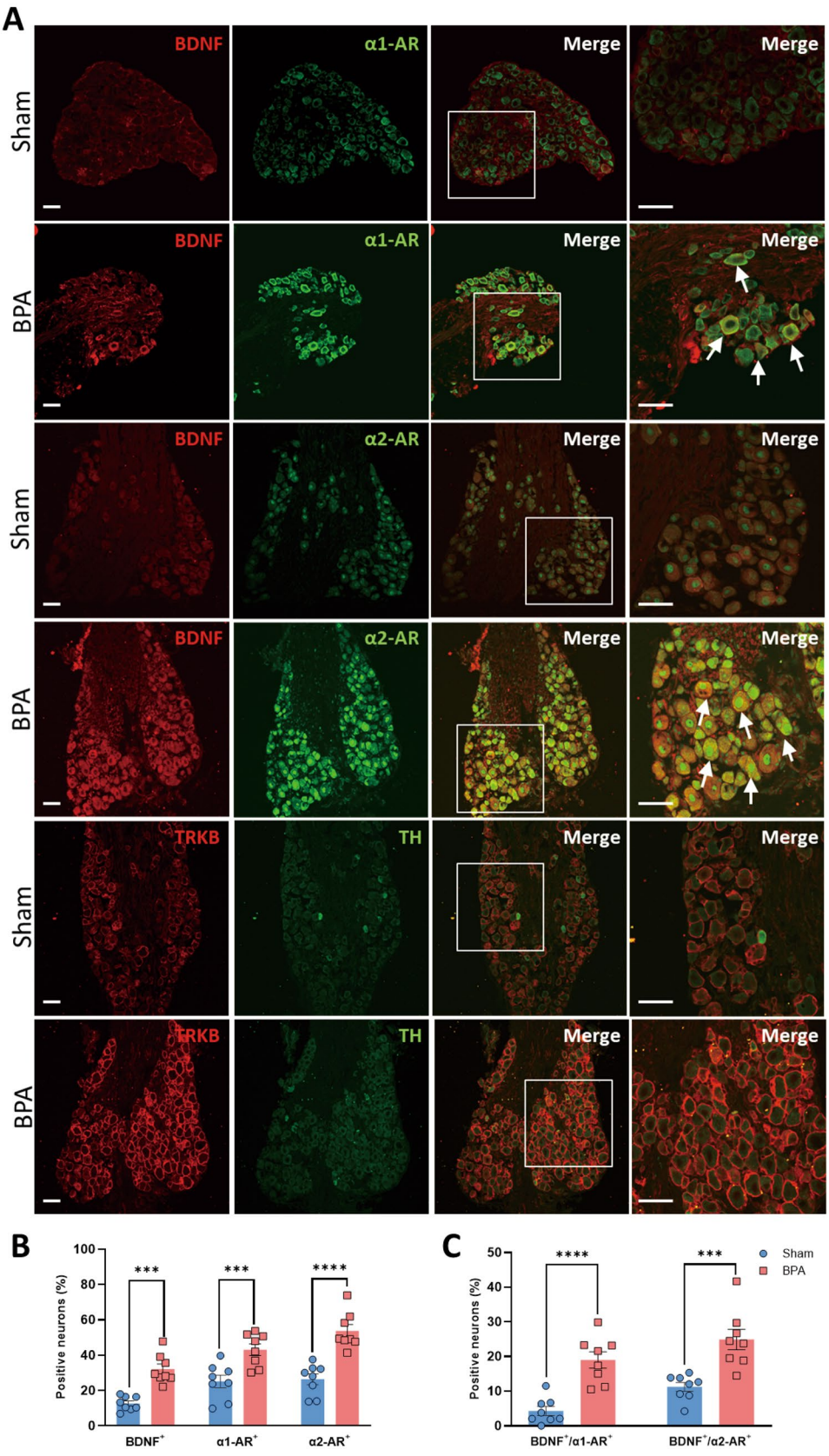

Fig. 3 Immunofluorescence labeling shows the elevated expression of NP markers (BDNF and TrκB) and SNS activity markers (α1-AR and α2-AR) in the ipsilateral DRGs of BPA mice. **A** Representative confocal images of BDNF (red), α1-ARs (green), α2-ARs (green), TrκB (red), and TH (green) in the DRG tissue of sham and BPA mice using immunofluorescence labeling. Higher fluorescence of BDNF, α1-ARs, α2-ARs, and TrκB is observed in the BPA group. **B** Analysis shows more BDNF-, α1-AR-, and α2-AR-positive neurons after BPA. **C** Analysis shows higher co-localization of BDNF/α-AR-positive neurons after BPA. Data are presented as the mean ± SEM. $^{***}P < 0.001$, $^{****}P < 0.0001$, *vs.* Sham. Scale bars, 50 μm. White arrows: co-localized neurons.

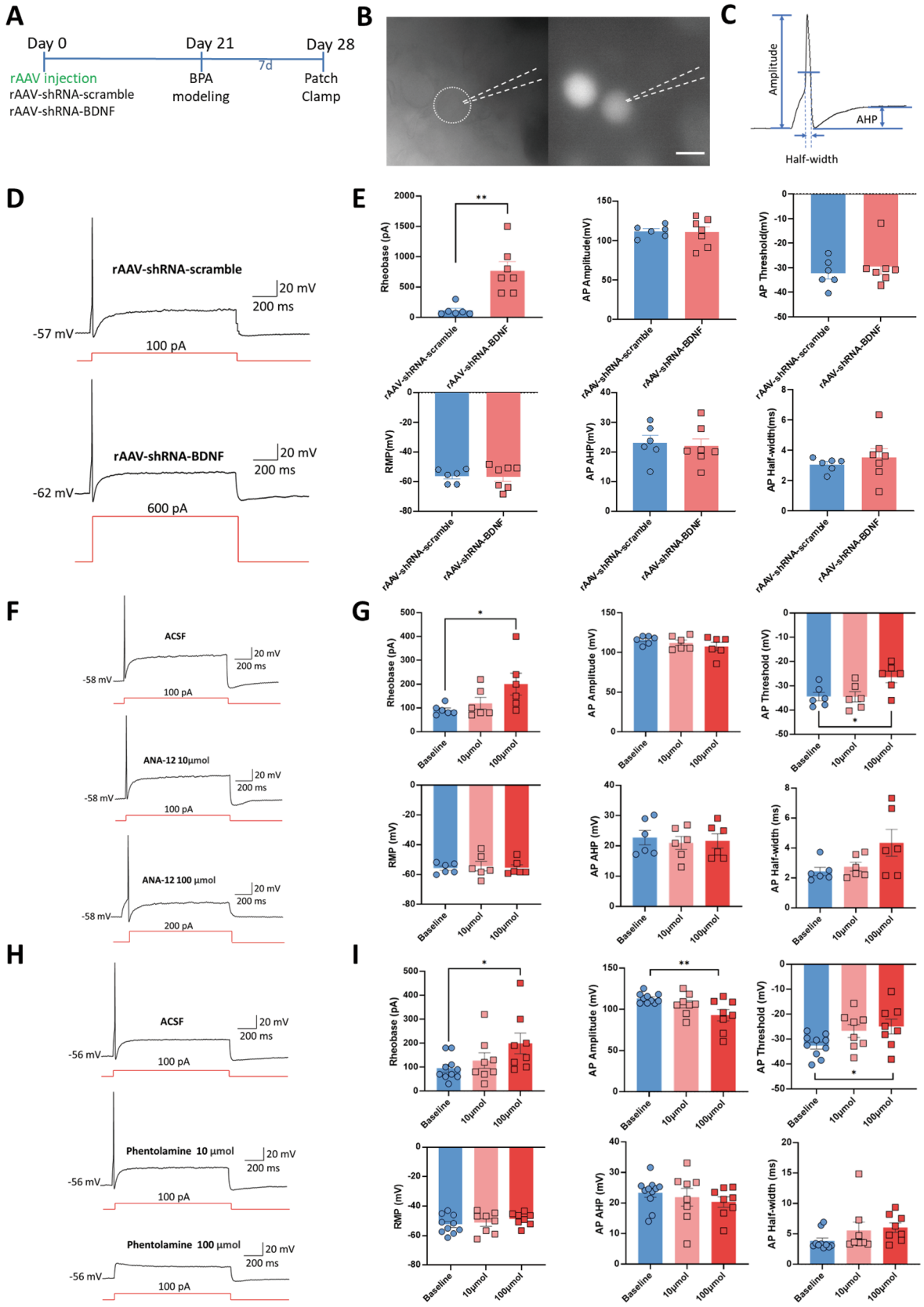
A
Day 0
Day 21
Day 28
7d
rAAV injection
rAAV-shRNA-scramble
rAAV-shRNA-BDNF
BPA modeling
Patch Clamp
B
C
Amplitude
AHP
Half-width
D
rAAV-shRNA-scramble
20 mV
200 ms
-57 mV
100 pA
rAAV-shRNA-BDNF
-62 mV
600 pA
E
Rheobase (pA)
AP Amplitude(mV)
AP Threshold(mV)
RMP(mV)
AP AHP(mV)
AP Half-width(ms)
rAAV-shRNA-scramble
rAAV-shRNA-BDNF
F
ACSF
-58 mV
ANA-12 10μmol
ANA-12 100 μmol
200 pA
G
Rheobase (pA)
AP Amplitude (mV)
AP Threshold (mV)
RMP (mV)
AP AHP (mV)
AP Half-width (ms)
Baseline
10μmol
100μmol
H
-56 mV
Phentolamine 10 μmol
Phentolamine 100 μmol
I

◂**Fig. 4** Both genetic knockdown of BDNF in DRGs and the use of antagonists of TrκB and α-ARs reverse the hyperexcitation of DRG neurons in BPA mice. **A** Schematic showing BPA modeling was performed on day 21 after virus delivery and patch clamp recording was performed on day 7 after BPA. **B** Representative images of the single-cell patch with fluorescence expression. **C** Representative trace of an action potential (AP) and marked analytical metrics. **D** Representative traces of AP in the rAAV-shRNA-scrambled and rAAV-shRNA-BDNF groups. Neurons in the rAAV-shRNA-BDNF group need stronger stimulation (600 pA) for firing. **E** Knockdown of BDNF in DRG increases the rheobase of DRG neurons after BPA but has little effect on the AP amplitude, AP threshold, resting membrane potential (RMP), AP afterhyperpolarization potential (AHP), and AP half-width. **F** Representative traces of APs in ANA-12-treated groups, including ACSF, 10 μmol, and 100 μmol ANA-12 groups. At 100 μmol, neurons need stronger stimulation (200 pA) for firing. **G** Delivery of 100 μmol ANA-12 increases the rheobase and AP threshold of DRG neurons after BPA but has little effect on the AP amplitude, RMP, AP AHP, and AP half-width. Delivery of 10 μmol had no effect on the above metrics. **H** Representative traces of APs in phentolamine-treated groups, including ACSF, 10 μmol, and 100 μmol phentolamine groups. Phentolamine at 100 μmol inhibits the firing of neurons. **I** Delivery of 100 μmol phentolamine increases the rheobase and AP threshold, and decreases the AP amplitude of DRG neurons after BPA, but has little effect on the RMP, AP AHP, and AP half-width. Data are presented as the mean ± SEM. $*P < 0.05$, $**P < 0.01$, *vs.* rAAV-shRNA-scrambled or baseline. Scale bar, 50 μm.

BPA Increases the Overexpression of BDNF and Sympathetic Nerve Activity-Related Molecules in the Mouse DRG

To further investigate the molecular mechanism underlying this pathophysiological process, we used western blots to assess the NP markers BDNF and TrκB, and the SNS activity markers tyrosine hydroxylase (TH), α1-AR, and α2-AR. The results showed that the expression of BDNF and its high-affinity receptor TrκB was elevated on day 7 after BPA, and the expression of α1-AR and α2-AR increased at the same time, which was significantly different from the sham group ((Fig. 2A, B). Meanwhile, the expression of the sympathetic nerve marker TH did not significantly differ from the sham group (Fig. 2A, B). The following immunofluorescence labeling tests showed that the fluorescence of BDNF, TrκB, α1-AR, and α2-AR in the ipsilateral DRGs of the BPA group was stronger than that in the sham group (Fig. 3A, B). The neurons with enhanced BDNF expression also had higher co-localization fluorescence labeling with α-ARs; this builds a structural basis for the interaction between the somatosensory and sympathetic nervous systems (Fig. 3C). In the meantime, the co-localization of BDNF/α-ARs in CGRP- and IB4 positive neurons showed that BDNF tended to have more co-expression in CGRP-positive neurons after BPA (Figs. S2, S3). These results indicated that peptidergic neurons in DRG were more responsive to the perception of pain after BPA.

Regulation of BDNF, TrκB, and Adrenergic Receptors Reduces the Activity of DRG Neurons

Patch-clamp recording is a direct method of evaluating the state of excitability of target neurons. To evaluate the effect of BDNF expression on the activity of neurons, we used rAAV-carried shRNA to knock down the expression of BDNF in DRGs. Three weeks after the virus injection, the BPA model was created. Seven days after BPA, the ipsilateral DRG at C6 or C8 was removed and recorded (Fig. 4A). Neurons carrying fluorescence were recorded in the virus-injection groups (Fig. 4B), and the amplitude, half-width, and afterhyperpolarization potential (AHP) were analyzed based on representative action potentials (APs) (Fig. 4C). Compared with the rAAV-shRNA-scrambled group, the APs of neurons in the BDNF knockdown group (rAAV-shRNA-BDNF) needed stronger stimulation (600 pA) to be activated, and the rheobase was significantly increased in this group; the AP amplitude, AP threshold, RMP, AP AHP, and AP half-width did not significantly differ between the two groups (Fig. 4D, E). These results showed that the knockdown of BDNF reduced the excitability of the DRG neurons affected by BPA injury. Next, to explore the interaction between somatosensory and sympathetic nervous systems, the TrκB antagonist ANA-12 and the α-AR antagonist phentolamine were used during recordings. Under the same stimulation mode (100 pA), ANA-12 at 100 μmol inhibited the firing of neurons and increased the rheobase and AP threshold, which reduced the excitability of the affected DRG neurons; stronger stimulation (200 pA) induced APs with ANA-12 at 100 μmol (Fig. 4F, G). Interestingly, the use of the α-AR antagonist phentolamine at 100 μmol gave results similar to ANA-12, in that the rheobase and AP threshold were increased and the AP amplitude was decreased (Fig. 4H, I). This result indicated that regulation of the SNS can directly affect the activity of the somatosensory nervous system. While a lower concentration of ANA-12 and phentolamine (10 μmol) had little effect on the target neurons. Surprisingly, in the ANA-12 group, we recorded one neuron that discharged multiple spikes after depolarization, and the number of spikes was reduced at the low concentration (10 μmol), and more at the higher concentration (100 μmol) (Fig. S4). This indicates the participation of another type of neuron in the process of BPA, which also sheds light on further investigation of the mechanisms of different types of neurons in BPA-induced NP.

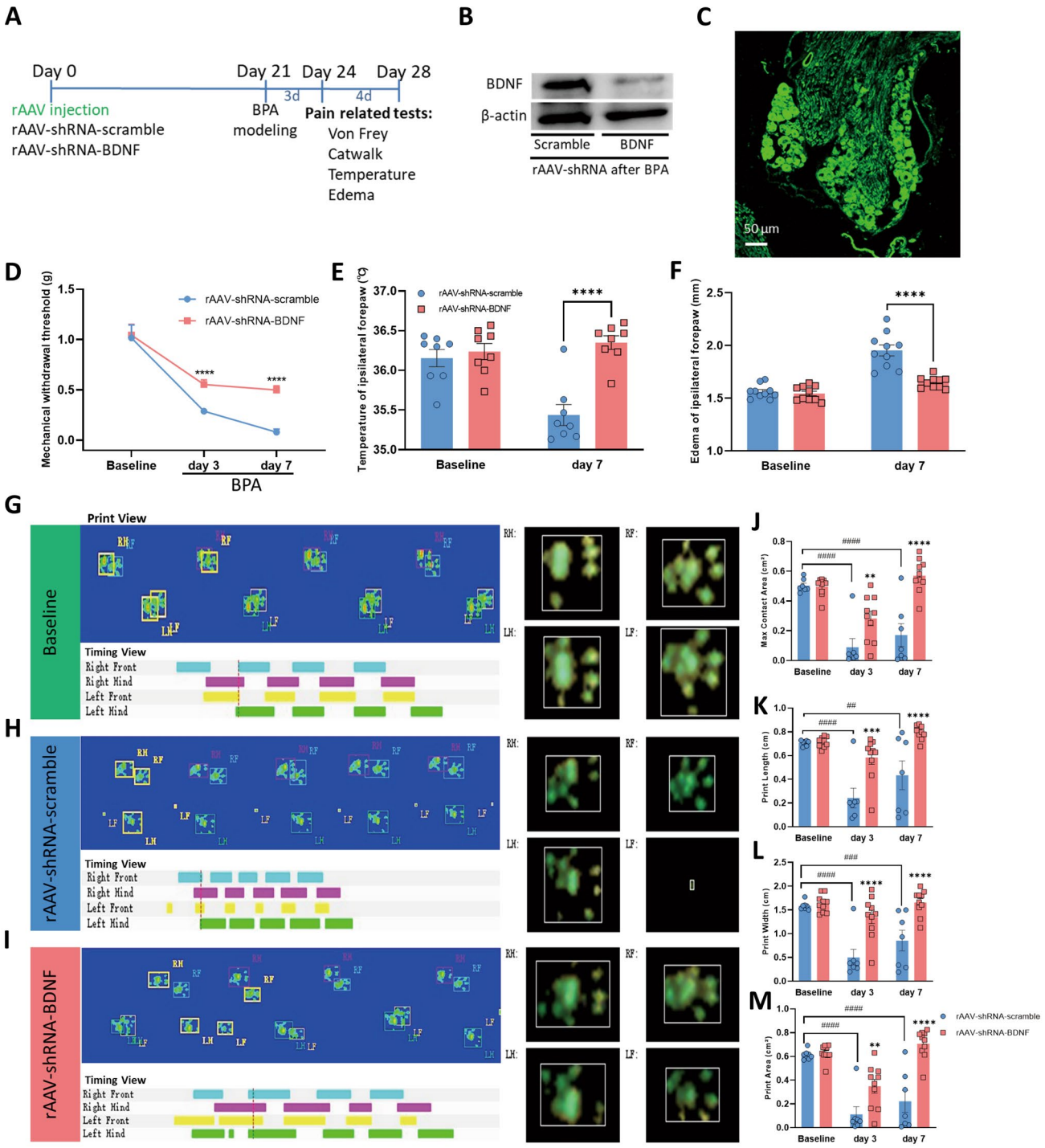

Fig. 5 Genetic knockdown of BDNF in DRGs relieves the mechanical allodynia and symptoms of sympathetic nerve hyperexcitability in BPA mice. **A** Schematic showing rAAV delivery groups and following tests. **B** Typical western blot images of BDNF knockdown in the DRG tissue of BPA mice. **C** Confocal image of BDNF knockdown virus injected into the DRG (EGFP). **D–F** BDNF knockdown in the DRG increases the mechanical allodynia threshold (**D**), relieves the hypothermia (**E**), and relieves the edema (**F**) in the ipsilateral forepaw of BPA mice, $n = 8–10$. **G–I** Representative images of CatWalk gait including print view, timing view, and foot view of mice in the rAAV-shRNA-scrambled and rAAV-shRNA-BDNF groups. **J–M** The max contact area, print length, print width, and print area decreases after BPA in the rAAV-shRNA-scrambled group, and this was reversed through BDNF knockdown in the DRG, both on day 3 and day 7 after BPA. This indicates pain and sympathetic nerve hyperexcitability can be controlled by BDNF knockdown. Data are presented as the mean ± SEM. $^{*}P < 0.05$, $^{**}P < 0.01$, $^{***}P < 0.001$, $^{****}P < 0.0001$, *vs.* rAAV-shRNA-scrambled. $^{\#\#}P < 0.01$, $^{\#\#\#}P < 0.001$, $^{\#\#\#\#}P < 0.0001$, *vs.* rAAV-shRNA-scrambled. RF, right forepaw; RH, right hind paw; LF, left forepaw; LH, left hind paw. Scale bar, 50 μm.

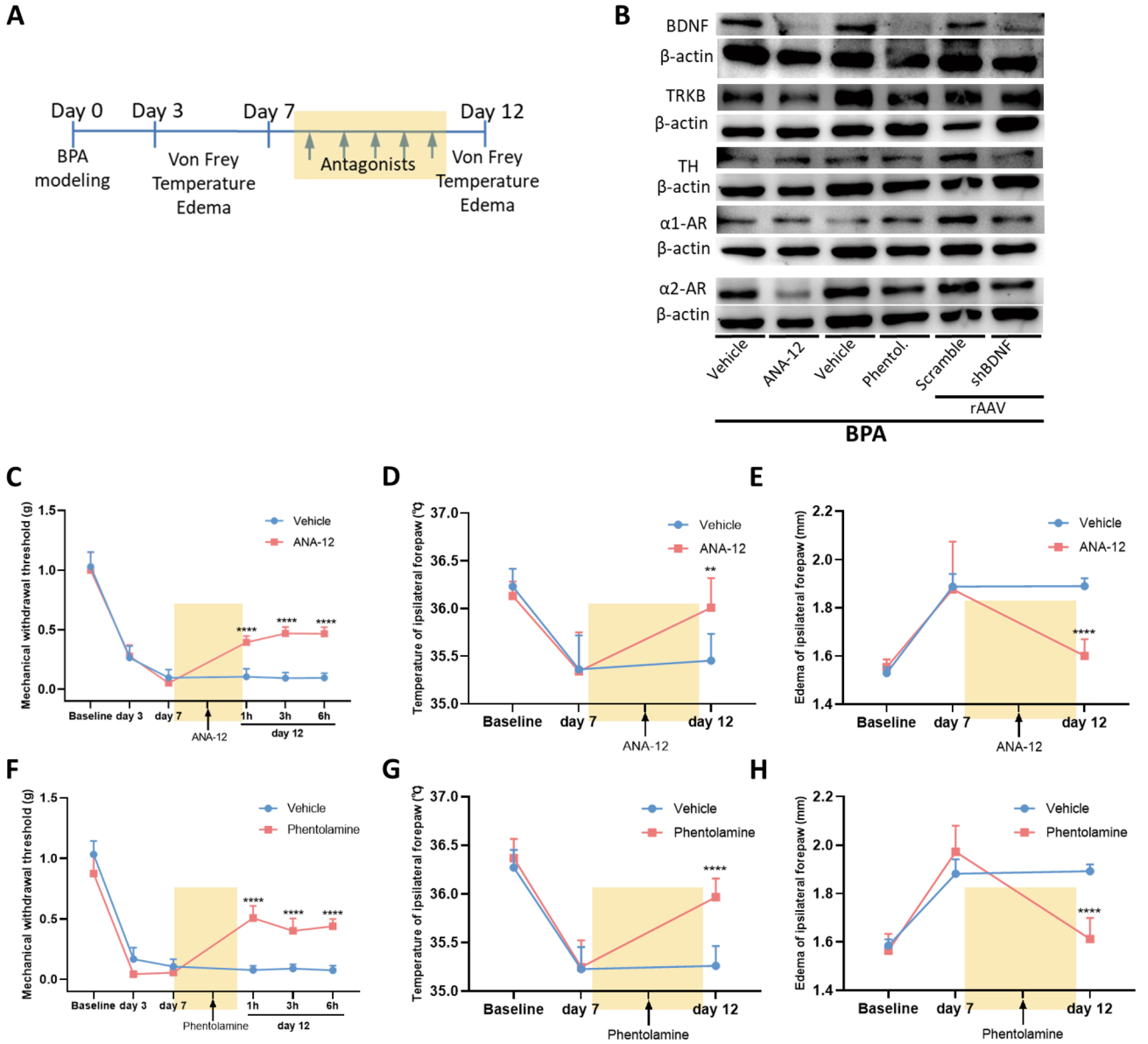

Fig. 6 Antagonists of TrκB and α-ARs relieve the mechanical allodynia and symptoms of sympathetic nerve hyperexcitability in BPA mice and reduce the expression of somatosensory-sympathetic coupling-related molecules. **A** Schematic showing the antagonist delivery groups and following tests. Antagonists are started on day 7 after BPA, and then once a day for 5 consecutive days. **B** Typical western blots showing BDNF knockdown in the DRG tissue of BPA and intraperitoneal (i.p.) injection of antagonists (ANA-12 and phentolamine). **C, F** Mechanical allodynia threshold of the affected ipsilateral forepaw is increased by i.p. injection of ANA-12 and phentolamine, and the analgesic effect lasts for 6 h after BPA. **D, G** Injection of ANA-12 and phentolamine relieve the hypothermia in the ipsilateral forepaw of mice after BPA. **E, H** Injection of ANA-12 and phentolamine relieve the edema in the ipsilateral forepaw of mice after BPA. Data are presented as the mean ± SEM. $^{**}P < 0.01$, $^{****}P < 0.0001$, *vs.* vehicle group. $n = 8$ per group.

Regulation of the BDNF, TrκB, and Adrenergic Receptors Relieves the Mechanical Allodynia and Attenuates the Activity of Sympathetic Nerves

The above results showed that regulation of BDNF through knockdown and an antagonist decreased the excitability of DRG neurons after BPA and the presence of somatosensory-SNS crosstalk. Whether this regulation could affect the behavioral results to ease pain and its underlying molecular mechanism remains unclear. Three weeks after the virus injection, the BPA model was created. Pain-related tests were conducted 3 and 7 days after BPA (Fig. 5A). After completion of the

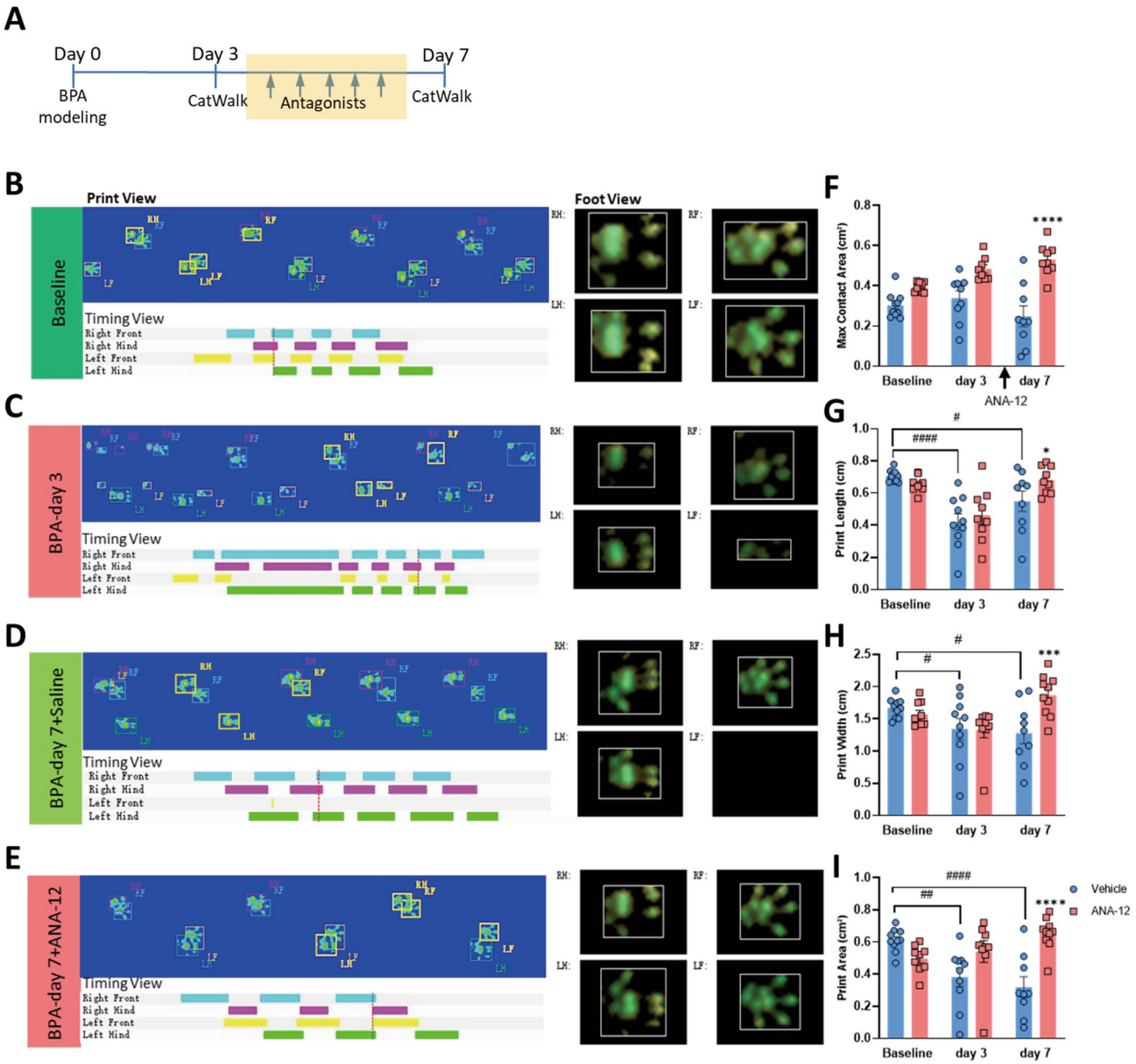

Fig. 7 Gait analysis shows that antagonists of TrκB and α-ARs relieve the mechanical allodynia and symptoms of sympathetic nerve hyperexcitability in BPA mice. **A** Schematic showing the antagonist delivery groups and following gait analysis. Antagonists were started on day 3 after BPA, and then once a day for 5 consecutive days. **B–E** Representative images of CatWalk gait including print view, timing view, and foot view of mice in the vehicle and ANA12 groups. **F–I** The print length, print width, and print area decreases after BPA in the vehicle group, and this is reversed by ANA12 injection on day 7 after BPA. (**J-M**) Representative images of CatWalk gait including print view, timing view, and foot view of mice in the vehicle and phentolamine groups. **N–Q** The max contact area decreases remarkably in the vehicle group and this is reversed by phentolamine injection on day 7 after BPA. Phentolamine has little effect on the print length, print width, and print area of BPA mice. Data are presented as the mean ± SEM. $^{*}P < 0.05$, $^{***}P < 0.001$, $^{****}P < 0.0001$, *vs.* vehicle group, $^{\#}P < 0.05$, $^{\#\#}P < 0.001$, $^{\#\#\#\#}P < 0.0001$, *vs.* vehicle group. RF, right forepaw; RH, right hind paw; LF, left forepaw; LH, left hind paw.

behavioral tests, DRGs were collected and western blot analysis was applied. The western blot and immunofluorescence results showed the effectiveness of viral interference (Fig. 5B, C). Knockdown of the expression of BDNF in DRG relieved the mechanical allodynia on days 3 and 7 after BPA (Fig. 5D), and the hyperexcitation of SNS symptoms (hypothermia and edema) of the affected forepaw were also improved (Fig. 5E, F). The gait analysis showed that the max contact area, print

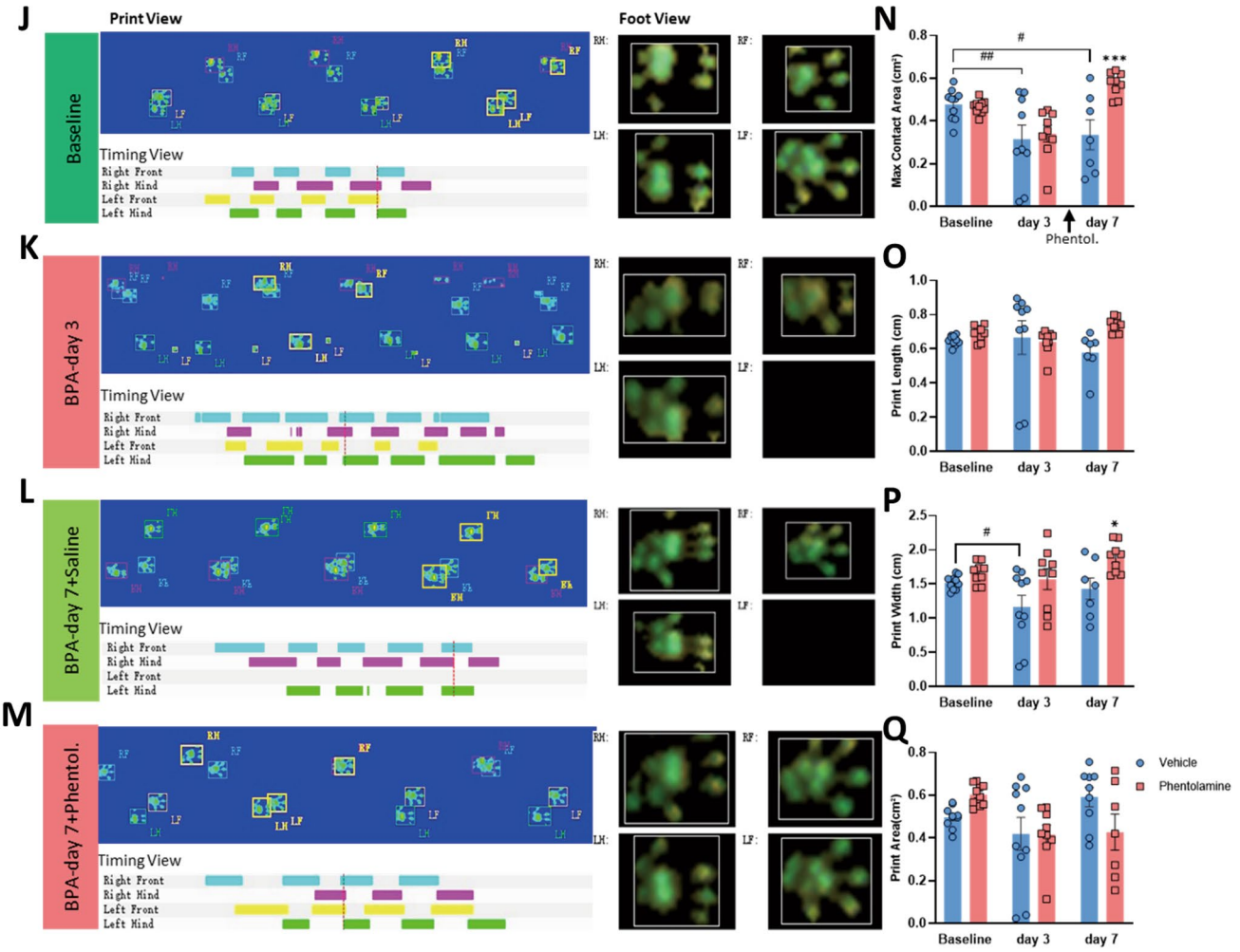

Fig. 7 (continued)

length, print width, and print area were all improved both on day 3 and day 7 after BPA in the rAAV-shRNA-BDNF group (Fig. 5G–M). Both stand and max contact mean intensity increased after BDNF knockdown on days 3 and 7 after BPA, and body speed and run average speed increased on day 7 after BPA in the rAAV-shRNA-BDNF group (Fig. S5A). Administration of ANA12 and phentolamine for 5 days (once a day, starting on day 7 after BPA, Fig. 6A) relieved the mechanical allodynia, hypothermia, and edema of the affected forepaw on day 12 after BPA (Fig. 6C–H). In the gait analysis groups, the BPA model was created after baseline recording and antagonist administration started on day 3 after BPA (once a day for 5 days, Fig. 7A). The results in the ANA-12 group showed that the max contact area, print length, print width, and print area were all improved on day 7 after BPA (Fig. 7B–I). The max contact mean intensity increased after ANA-12 use while standing, body speed, and run average speed showed no change (Fig. S5B). Administration of phentolamine for 5 days showed that the max contact area improved on day 7 after BPA, while the other parameters showed no difference (Figs. 7J–Q, S5C).

Additional molecular tests using western blots showed that knockdown of BDNF in the DRG decreased the expression of TH, α1-AR, and α2-AR, using ANA12 decreased the expression of BDNF, TrκB, and α2-AR, and using phentolamine decreased the expression of BDNF, TrκB, and α2-AR after BPA (Fig. 6B). These results indicate that regulation strategies of both the somatosensory and sympathetic nervous systems can achieve the goal of pain and sympathetic activity regulation bidirectionally, especially through the gene regulation of BDNF at the peripheral level. Genetic ablation of BDNF at the peripheral level had a stronger effect on the regulation of this pathological process. Therefore, the existence of somatosensory-SNS crosstalk was also clearly demonstrated here, and BDNF plays a crucial role during this process.

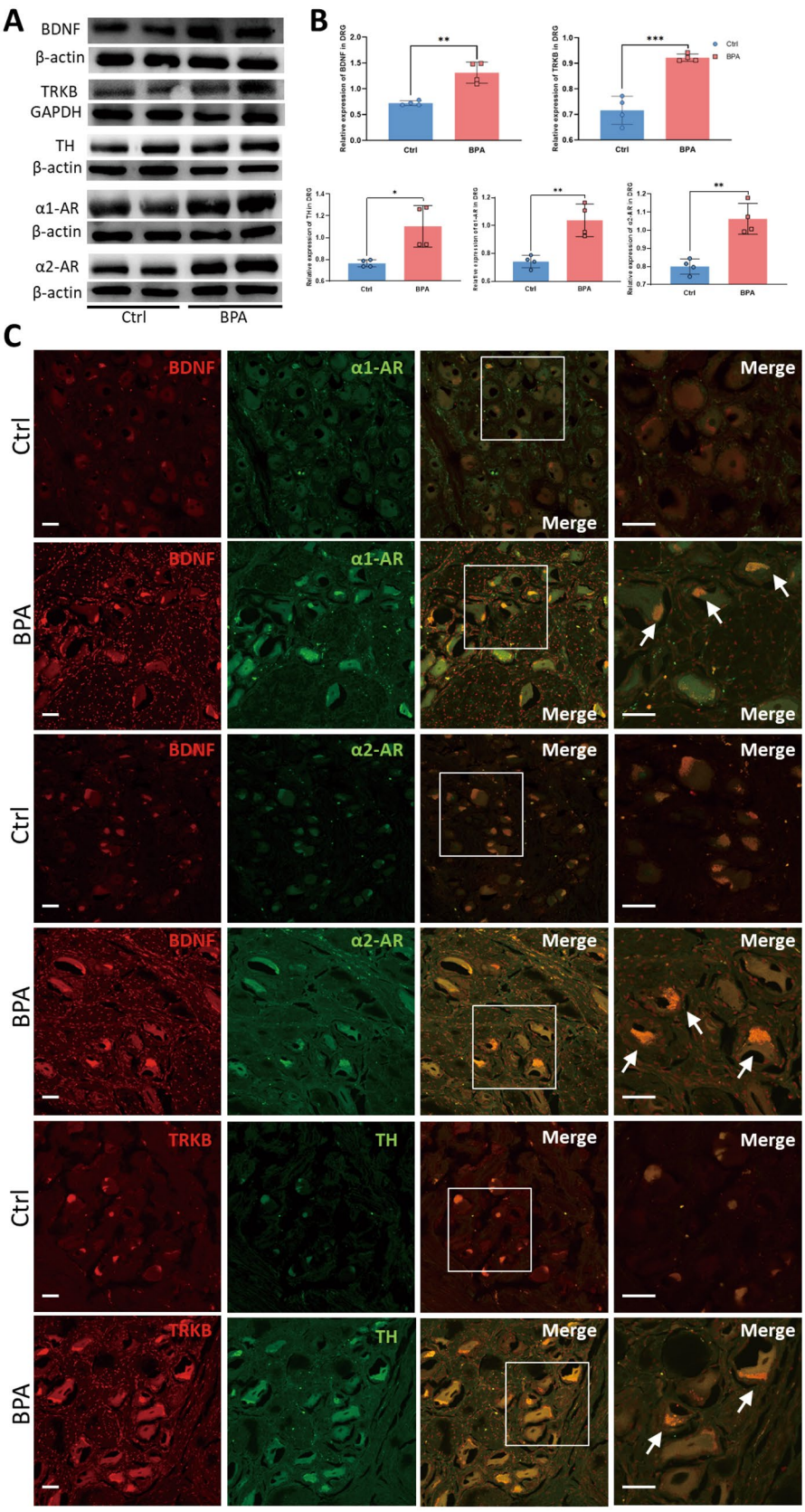

Fig. 8 Expression of BDNF, TrκB, TH, α1-ARs, and α2-ARs are increased in the avulsed DRGs of clinical BPA patients. **A** Typical Western blots and quantitative summary levels of BDNF, TrκB, TH, α1-ARs, and α2-ARs in the DRG tissue of control and human BPA samples. Data are normalized to the housekeeping protein β-actin or GAPDH. **B** BPA increases the expression of BDNF, TrκB, TH, α1-ARs, and α2-ARs in the DRG of humans. **C** Representative confocal images of BDNF (red), α1-ARs (green), α2-ARs (green), TrκB (red), and TH (green) in the DRG tissue of control and human BPA samples using immunofluorescence labeling. Data are presented as the mean ± SEM. $^{*}P < 0.05$, $^{**}P < 0.01$, $^{***}P < 0.001$, *vs.* Ctrl. Scale bars, 50 μm. White arrows: co-localized neurons.

DRGs from BPA Patients Show Molecular Expression Changes Similar to BPA Mouse Models

To explore the molecular changes of avulsed DRGs from BPA-induced NP patients, the NP markers (BDNF and TrκB) and SNS activity markers (TH, α1-ARs, and α2-ARs) were tested in the tissue collected from normal human (Control group) and BPA patients (BPA group). The western blot results showed the expression of BDNF and its high-affinity receptor TrκB were elevated in BPA patients' DRGs, and the expression of TH, α1-ARs, and α2-ARs increased at the same time; these were significantly different from the Control group (Fig. 8A, B). As only avulsed roots could be collected from BPA patients, we further tested the BDNF expression in the avulsed C7 root of BPA mice. The results showed increased expression of BDNF in BPA patients (Fig. S6). The following immunofluorescence labeling tests showed that the fluorescence of BDNF, TrκB, α1-ARs, and α2-ARs in the BPA group was stronger than in the Control group (Fig. 8C). The proportion of BDNF- and α-AR-positive neurons increased in BPA patients, and the neurons with enhanced BDNF expression also had high co-localization fluorescence labeling with α-ARs according to quantitative analysis (Fig. S7). The changes at the molecular level of BPA patients have a pattern similar to BPA mice, which indicates the presence and structural basis for the interaction between somatosensory and sympathetic nervous systems at the peripheral DRG level in humans.

Discussion

Brachial plexus avulsion (BPA) can induce severe neuropathic pain (NP) in patients, and this novel mouse model can mimic the pathophysiological processes in BPA patients due to similar destruction of the somatosensory pathway. The single C7 root avulsion model (BPA model) showed persistent mechanical allodynia of the affected limb, and the SNS was then activated, followed by the symptoms of hypothermia and edema. These somatosensory-sympathetic activity symptoms are paralleled by BPA patients in the clinic. Then, to further investigate the underlying mechanism, we found the overexpression of BDNF (a marker of somatosensory activity) and α1-ARs and α2-ARs (indirect markers of sympathetic activity) in the DRG of BPA mice and patients. The direct sympathetic activity marker TH also increased in the DRG of BPA patients. Next, genetic knockdown of BDNF and medication to inhibit the TrκB and α-ARs not only reversed the hyperexcitation of the neurons but also alleviated the mechanical allodynia and reduced the sympathetic activity. Our results demonstrated the crosstalk between the somatosensory and sympathetic nervous systems in BPA-induced NP, and the crosstalk at the DRG level contributes to the development of peripheral sensitization through BDNF signaling.

The SNS has been shown to participate directly in pain conditions [17, 26–28]. Sensory neurons in the DRG are not normally innervated by the SNS, while several preclinical pain models have described the sympathetic innervation of DRGs under pathological conditions [29–31]. The sympathetic fibers form a dense plexus in a basket structure around individual neurons has been reported both in pain models and also in humans with NP [26, 32]. This basket structure has been shown to be the structural basis of direct somatosensory-sympathetic coupling during a pain state. In this study, we did not detect typical basket structures in the DRG of the BPA model or BPA patients, as Nascimento *et al.* [33] previously reported that sympathetic fibers do not sprout into the DRG at 2 or 6 weeks in the cuff and spared nerve injury (SNI) models. However, the expression of the marker of sympathetic nerves (TH) was confirmed through western blots and immunofluorescence labeling both in mice and humans, which indicated the presence of sympathetic fibers in the affected DRGs. Furthermore, the increased expression of TH after BPA in the human DRG indicates it may take a longer time due to the structural plasticity of sympathetic sprouting.

Sympathetic nerve fiber endings release NE to participate in many physiological processes. Under normal conditions, the function of these fibers is related to blood vessel regulation in the DRG, and they have been shown to communicate with somatosensory nerves after nerve injury [34]. NE is thought to contribute to the maintenance of pain through ARs, while the effects of different types of AR on pain are still controversial [35]. All ARs, including α- and β-ARs, are expressed in DRGs, and accumulating evidence has demonstrated the participation of ARs in the pathophysiology of pain. Both α1- and α2-ARs are known to affect the excitability of DRG neurons in pain [35, 36]. Shen *et al.* [26] found the involvement of β2-AR-mediated signaling in the satellite glial cells of DRGs in the sympathetic modulation of sensory activity and chronic pain. Meanwhile, sympathetic blocks using a non-selective α-AR antagonist (phentolamine) can relieve pain through the possible mechanism that α-AR blockers reduce the pain sensation that arises from noradrenergic nociception based on clinical data [12]. In the current study, α-ARs, including the α1 and α2 subtypes, were found to increase both in BPA models and patients; this can be treated as evidence of a change in sympathetic nerve sensitivity. Ji *et al.* [35] reported co-expression of α1- and α2-ARs in the same peripheral neurons, indicating that NE released from sympathetic sprouts exerts its effect on the receptor-positive neurons after SNI. α-ARs also show elevated expression in humans with pain [15]. This elevated expression of α-ARs could be treated as

another form of hyperexcitation responses of neurons to sympathetic nerves, which makes neurons more sensitive to transmitters (NE) released by sympathetic endings and could be termed adrenergic supersensitivity. Using a non-selective α-AR antagonist (phentolamine) not only can regulate the function of sympathetic nerve fibers but also reverse the hyperexcitation of DRG neurons.

Several mediators are critical in the initiation and maintenance of pain. Molecular phenotype changes in DRGs, including by inflammation mediators (TNF-α, IL-1β, and ATP), neurotransmitters/growth factors (NGF, BDNF, and GDNF), and ion channels (Na_v and K_v), can facilitate the process of pain [37]. Meanwhile, little is known about the molecular basis of somatosensory and sympathetic coupling, especially in BPA. It has been reported that NE acts directly on DRG neurons to inhibit the activity of TRPV1 (transient receptor potential vanilloid 1) through the activation of α2-ARs [38], while modulation of P2X receptors *via* adrenergic pathways by activating α1-ARs is responsible for noradrenergic sprouting after SNI [39]. To search for the molecule regulating the somatosensory-sympathetic coupling under BPA-induced NP, we found that the expression of BDNF and its high-affinity receptor (TrκB) increased after BPA in mice. BDNF plays a key role in cell growth, differentiation, maturation, and synapse formation [40, 41]. Previous studies have shown that DRGs can actively synthesize and release BDNF, and they can bind to its receptors on the cell surface of neurons, resulting in hyperexcitation of the neurons and participating in peripheral sensitization under NP [42, 43]. Genetic ablation of BDNF in DRGs after BPA not only alleviated the mechanical allodynia but also relieved the edema and hypothermia of the affected forepaw, and the use of the TrκB antagonist ANA12 and α-AR antagonist phentolamine can also regulate the activity of each other bidirectionally. Direct recording of the excitation of neurons also revealed the crosstalk between somatosensory and sympathetic nervous systems; phentolamine reversed the hyperexcitation of neurons after BPA, similar to ANA-12. Following molecular changes after the above regulation provided stronger evidence of this functional coupling, including that knockdown of BDNF decreased the expression of TH and α-ARs. Another striking finding of the present study was the similar pattern of overexpression of BDNF in DRGs from BPA patients, which further confirmed the participation of BDNF in this pain process as in other human-related reports [44, 45]. These results imply that peripheral BDNF plays a key role in regulating both sensitization and somatosensory-sympathetic coupling at the peripheral level. Targeting BDNF may be a potential therapeutic method for treating BPA-induced NP and related sympathetic comorbidities, which has great potential for clinical application.

The current study also presents a limitation that only female mice were used. As more and more studies have identified the existence of gender-associated differences in pain sensation and related mechanisms [46, 47], we used only female mice to avoid the potential influence of gender issues on pain and related complications or mechanisms. Additional further investigations are needed to test whether male mice share a similar somatosensory-sympathetic coupling mechanism as females in the BPA-induced pain state.

In summary, our study demonstrated that sympathetic nerve fibers interact with sensory neurons through BDNF signaling at the peripheral level in the BPA model and in patients, and is a crucial mechanism of the formation of peripheral sensitization. Peripheral BDNF could be a peripheral therapeutic candidate for treating BPA-induced NP with fewer side-effects than systemic medication or central nervous treatment. Unlike other NP conditions, few previous efforts have explored the NP mechanism based on BPA animal models. The consistent findings based on rodents and humans in this study provide a crucial stepping stone for future translation, while the complex underlying mechanism of BPA-induced NP still needs further deep mining.

Acknowledgments This work was supported by grants from the National Natural Science Foundation of China (82072526, 82171212, and 81870867).

Data availability The original contributions presented in the study are included in the article, and further inquiries can be directed to the corresponding authors.

Conflict of interest All authors declare that there are no conflicts of interest.

References

1. Noland SS, Bishop AT, Spinner RJ, Shin AY. Adult traumatic brachial plexus injuries. J Am Acad Orthop Surg 2019, 27: 705–716.
2. Xian H, Xie R, Luo C, Cong R. Comparison of different *in vivo* animal models of brachial plexus avulsion and its application in pain study. Neural Plast 2020, 2020: 8875915.
3. Rodrigues-Filho R, Santos AR, Bertelli JA, Calixto JB. Avulsion injury of the rat brachial plexus triggers hyperalgesia and allodynia in the hindpaws: A new model for the study of neuropathic pain. Brain Res 2003, 982: 186–194.
4. Le W, Liu Y, Zhou Y, Lao J, Zhao X. A new rat model of neuropathic pain: Complete brachial plexus avulsion. Neurosci Lett 2015, 589: 52–56.
5. Pace MC, Passavanti MB, De Nardis L, Bosco F, Sansone P, Pota V. Nociceptor plasticity: A closer look. J Cell Physiol 2018, 233: 2824–2838.

6. Luo C, Kuner T, Kuner R. Synaptic plasticity in pathological pain. Trends Neurosci 2014, 37: 343–355.
7. Kong YF, Sha WL, Wu XB, Zhao LX, Ma LJ, Gao YJ. CXCL10/CXCR3 signaling in the DRG exacerbates neuropathic pain in mice. Neurosci Bull 2021, 37: 339–352.
8. Wang F, Ma SB, Tian ZC, Cui YT, Cong XY, Wu WB, *et al*. Nociceptor-localized cGMP-dependent protein kinase I is a critical generator for central sensitization and neuropathic pain. Pain 2020, 162: 135–151.
9. Ma SB, Xian H, Wu WB, Ma SY, Liu YK, Liang YT, *et al*. CCL2 facilitates spinal synaptic transmission and pain *via* interaction with presynaptic CCR2 in spinal nociceptor terminals. Mol Brain 2020, 13: 161.
10. Wang K, Wang S, Chen Y, Wu D, Hu X, Lu Y, *et al*. Single-cell transcriptomic analysis of somatosensory neurons uncovers temporal development of neuropathic pain. Cell Res 2021, 31: 904–918.
11. Han WJ, Ma SB, Wu WB, Wang FD, Cao XL, Wang DH, *et al*. Tweety-homolog 1 facilitates pain *via* enhancement of nociceptor excitability and spinal synaptic transmission. Neurosci Bull 2021, 37: 478–496.
12. Phuphanich ME, Convery QW, Nanda U, Pangarkar S. Sympathetic blocks for sympathetic pain. Phys Med Rehabil Clin N Am 2022, 33: 455–474.
13. Zhu X, Xie W, Zhang J, Strong JA, Zhang JM. Sympathectomy decreases pain behaviors and nerve regeneration by downregulating monocyte chemokine CCL2 in dorsal root ganglia in the rat tibial nerve crush model. Pain 2022, 163: e106–e120.
14. Chang C, McDonnell P, Gershwin ME. Complex regional pain syndrome - False hopes and miscommunications. Autoimmun Rev 2019, 18: 270–278.
15. Drummond PD. Sensory disturbances in complex regional pain syndrome: Clinical observations, autonomic interactions, and possible mechanisms. Pain Med 2010, 11: 1257–1266.
16. Zheng Q, Xie W, Lückemeyer DD, Lay M, Wang XW, Dong X, *et al*. Synchronized cluster firing, a distinct form of sensory neuron activation, drives spontaneous pain. Neuron 2022, 110: 209-220. e6.
17. Liu P, Zhang Q, Gao YS, Huang YG, Gao J, Zhang CQ. The delayed-onset mechanical pain behavior induced by infant peripheral nerve injury is accompanied by sympathetic sprouting in the dorsal root ganglion. Biomed Res Int 2020, 2020: 9165475.
18. Nascimento AI, Mar FM, Sousa MM. The intriguing nature of dorsal root ganglion neurons: Linking structure with polarity and function. Prog Neurobiol 2018, 168: 86–103.
19. Krames ES. The role of the dorsal root ganglion in the development of neuropathic pain. Pain Med 2014, 15: 1669–1685.
20. Sah DWY, Ossipo MH, Porreca F. Neurotrophic factors as novel therapeutics for neuropathic pain. Nat Rev Drug Discov 2003, 2: 460–472.
21. Zhang KL, Li SJ, Pu XY, Wu FF, Liu H, Wang RQ, *et al*. Targeted up-regulation of Drp1 in dorsal horn attenuates neuropathic pain hypersensitivity by increasing mitochondrial fission. Redox Biol 2022, 49: 102216.
22. Vieira WF, Malange KF, de Magalhães SF, dos Santos GG, de Oliveira ALR, da Cruz-Höfling MA, *et al*. Gait analysis correlates mechanical hyperalgesia in a model of streptozotocin-induced diabetic neuropathy: A CatWalk dynamic motor function study. Neurosci Lett 2020, 736: 135253.
23. Walter J, Kovalenko O, Younsi A, Grutza M, Unterberg A, Zweckberger K. The CatWalk XT® is a valid tool for objective assessment of motor function in the acute phase after controlled cortical impact in mice. Behav Brain Res 2020, 392: 112680.
24. Shen S, Ding W, Ahmed S, Hu R, Opalacz A, Roth S, *et al*. Ultrasmall superparamagnetic iron oxide imaging identifies tissue and nerve inflammation in pain conditions. Pain Med 2018, 19: 686–692.
25. Zhang JL, Xian H, Zhao R, Luo C, Xie RG, Tian T, *et al*. Brachial plexus avulsion induced changes in gut microbiota promotes pain related anxiety-like behavior in mice. Front Neurol 2023, 14: 1084494.
26. Shen S, Tiwari N, Madar J, Mehta P, Qiao LY. Beta 2-adrenergic receptor mediates noradrenergic action to induce cyclic adenosine monophosphate response element-binding protein phosphorylation in satellite glial cells of dorsal root ganglia to regulate visceral hypersensitivity. Pain 2022, 163: 180–192.
27. Knudsen LF, Terkelsen AJ, Drummond PD, Birklein F. Complex regional pain syndrome: A focus on the autonomic nervous system. Clin Auton Res 2019, 29: 457–467.
28. Xie W, Strong JA, Zhang JM. Local knockdown of the $Na_V1.6$ sodium channel reduces pain behaviors, sensory neuron excitability, and sympathetic sprouting in rat models of neuropathic pain. Neuroscience 2015, 291: 317–330.
29. Xie W, Strong JA, Mao J, Zhang JM. Highly localized interactions between sensory neurons and sprouting sympathetic fibers observed in a transgenic tyrosine hydroxylase reporter mouse. Mol Pain 2011, 7: 53.
30. Xie W, Strong JA, Zhang JM. Localized sympathectomy reduces peripheral nerve regeneration and pain behaviors in 2 rat neuropathic pain models. Pain 2020, 161: 1925–1936.
31. Burton AR, Fazalbhoy A, Macefield VG. Sympathetic responses to noxious stimulation of muscle and skin. Front Neurol 2016, 7: 109.
32. Shinder V, Govrin-Lippmann R, Cohen S, Belenky M, Ilin P, Fried K, *et al*. Structural basis of sympathetic-sensory coupling in rat and human dorsal root ganglia following peripheral nerve injury. J Neurocytol 1999, 28: 743–761.
33. Nascimento FP, Magnussen C, Yousefpour N, Ribeiro-da-Silva A. Sympathetic fibre sprouting in the skin contributes to pain-related behaviour in spared nerve injury and cuff models of neuropathic pain. Mol Pain 2015, 11: 59.
34. Gierthmühlen J, Binder A, Baron R. Mechanism-based treatment in complex regional pain syndromes. Nat Rev Neurol 2014, 10: 518–528.
35. Yun Ji. Effect of sympathetic sprouting on the excitability of dorsal root ganglion neurons and afferents in a rat model of neuropathic pain. Biochem Biophys Res Commun 2022, 587: 49–57.
36. Perez DM. α_1-adrenergic receptors in neurotransmission, synaptic plasticity, and cognition. Front Pharmacol 2020, 11: 581098.
37. Guha D, Shamji MF. The dorsal root ganglion in the pathogenesis of chronic neuropathic pain. Neurosurgery 2016, 63: 118–126.
38. Matsushita Y, Manabe M, Kitamura N, Shibuya I. Adrenergic receptors inhibit TRPV1 activity in the dorsal root ganglion neurons of rats. PLoS One 2018, 13: e0191032.
39. Maruo K, Yamamoto H, Yamamoto S, Nagata T, Fujikawa H, Kanno T, *et al*. Modulation of P2X receptors *via* adrenergic pathways in rat dorsal root ganglion neurons after sciatic nerve injury. Pain 2006, 120: 106–112.
40. Camille S. Wang, BDNF signaling in context: From synaptic regulation to psychiatric disorders. Cell 2022, 185: 62–76.
41. Cao T, Matyas JJ, Renn CL, Faden AI, Dorsey SG, Wu J. Function and mechanisms of truncated BDNF receptor TrkB.T1 in neuropathic pain. Cells 2020, 9: 1194.
42. Lu VB, Biggs JE, Stebbing MJ, Balasubramanyan S, Todd KG, Lai AY, *et al*. Brain-derived neurotrophic factor drives the changes in excitatory synaptic transmission in the rat superficial dorsal horn that follow sciatic nerve injury. J Physiol 2009, 587: 1013–1032.
43. Kras JV, Weisshaar CL, Quindlen J, Winkelstein BA. Brain-derived neurotrophic factor is upregulated in the cervical dorsal root ganglia and spinal cord and contributes to the maintenance

of pain from facet joint injury in the rat. J Neurosci Res 2013, 91: 1312–1321.
44. Haberberger RV, Barry C, Dominguez N, Matusica D. Human dorsal root ganglia. Front Cell Neurosci 2019, 13: 271.
45. Middleton SJ, Barry AM, Comini M, Li Y, Ray PR, Shiers S, *et al*. Studying human nociceptors: From fundamentals to clinic. Brain 2021, 144: 1312–1335.
46. Vacca V, Marinelli S, de Angelis F, Angelini DF, Piras E, Battistini L, *et al*. Sexually dimorphic immune and neuroimmune changes following peripheral nerve injury in mice: Novel insights for gender medicine. Int J Mol Sci 2021, 22: 4397.
47. Lee SE, Greenough EK, Oancea P, Scheinfeld AR, Douglas AM, Gaudet AD. Sex differences in pain: Spinal cord injury in female and male mice elicits behaviors related to neuropathic pain. J Neurotrauma 2023, https://doi.org/10.1089/neu.2022.0482.